Ship wake detection using Radon transforms of filtered SAR imagery

Andrey Scherbakov*, Ramon Hanssen, George Vosselman
Delft University of Technology, Faculty of Geodetic Engineering
Delft, The Netherlands

Raymond Feron
Rijkswaterstaat, Survey Department
Delft, The Netherlands

ABSTRACT

Ship traffic surveillance plays an important role in providing safety of shipping, traffic management as well as treating a great deal of related environmental problems. One of the quite new but promising possibilities for this purpose lies in using satellite-borne Synthetic Aperture Radar (SAR) imagery. A moving ship produces a set of waves (ship wakes) often appearing in the image as bright or dark linear structures. These structures can provide information on both ship direction and speed. In the work presented here, the possibility of automatic detection of ship wakes was tested by applying the Radon transformation to the area surrounding the ship, followed by a verification of each detected wake by a set of criteria to discern it from other wake-like linear structures which are very often appearing in SAR imagery. Different methods for the improvement of the original image are applied as a preprocessing technique for the Radon transformation. The success of the algorithm implementation was found to depend greatly upon both wake and image appearances. The band-pass filtering together with a non-linear image amplification proved to be of use for the detection of practically invisible wakes.

1 INTRODUCTION

Gathering information about ship traffic is of importance for providing safety and efficiency of shipping as well as managing with a lot of urgent environmental problems. During the past 20 years all statistical data gathered by the responsible organization in Netherlands—the Directorate-General for Shipping and Maritime Affairs (DGSM)—have been obtained by direct aircraft visual observations.[2] This method is not only very expensive and time-consuming but also space-limited and failing to provide any information during bad weather conditions as well as during night time. The application of relatively new satellite methods using radar observations seems to be very promising for gathering information about ship traffic that is not so costly, systematic, and independent on time of the day and weather conditions.[1,2,5]

The work described here was performed in close collaboration with the Survey department of DGSM. With a future in which huge portions of information necessary for operational analysis of the situation need to be obtained, the manual treatment of the SAR-images will become very inefficient and time consuming. Therefore

*Currently at Moscow Institute of Physics and Technology, Dolgoprudny, Russia

the main purpose of the work consisted in development of an algorithm for automatic ship and wake recognition and the assessment of its possibilities.

All the images for the implementation of this work were provided by the Survey Department of DGSM and are extractions from ERS-1 SAR imagery taken over a part of the North Sea close to the North-West shore of the Netherlands during summer 1995.

The algorithm was based on the Radon transform of the original image. As most of the ships detectable in the SAR images are large ones and usually maintain a straight direction, the majority of the wakes also happen to be linear. The Radon transform of an image integrates values of the pixels along every line while each integral becomes a single point in the transform space. This process of averaging diminishes noise perturbations and hence increases the signal-to-noise ratio of the feature of interest. Due to this reason it has been considered as a quite appropriate method for the purpose of wake extraction. The description of the Radon transform is presented in the second part of this paper.

The application of Radon or Hough transforms for detections of ship wakes were investigated earlier by different authors.[5,1] Rey et al.[5] applied a running filter subtracting a local mean value from each pixel and a peak-shape detector based on the Wiener filter as pre- and post-processing techniques for wake detection improvement. In Copeland et al.,[1] the localized Radon transform and advantages of this method were discussed.

The position of a ship in the image is near but often displaced from its wake. This phenomenon is a result of the Doppler shift of the returned signal produced by the ship movement in the range direction. The returns from the ocean surface are not so significantly Doppler-shifted, and therefore the image of the wake itself is not displaced. This offset is very important as it provides all necessary information for evaluating the speed of the ship.

Due to their strong reflections, ships mostly appear in the SAR images as small areas of very bright pixels. The task of their detection in most cases can be resolved by simple thresholding. The situation in which a ship by some reason has no visible wakes is much more common than the contrary one.[4] Detection of the wakes represents a much more difficult problem, partly because of the great variety of appearances that wakes can have, and partly because of the presence of different kinds of noise and wake-like linear structures in the image.

The first problem arrives from the fact that the wake itself consists of many different components. These are the Kelvin wake, which itself consists of the cusp waves, the divergent waves and transverse waves; the turbulent wake; and possible narrow-V wake components.[5] In coastal areas—under certain conditions—there may also be ship-generated internal waves. In different situations only some of these wakes can be visible dependent upon the SAR sensor orientation as well as wind and water conditions. It should be mentioned that a wake can appear both darker or brighter than surrounding background in the image. Non-wake linear features are often generated by wind waves, salinity or thermal gradients, bottom topography, accumulations of algae and so on.

The whole idea and implementation of the wake detection is presented in the third part of the paper together with all the preliminary steps that are necessary for efficient algorithm performance.

The first results described in the fourth section show that in several cases the program could not reliably extract real wakes while returning a null result in its absence. Such situations were encountered mostly when wakes were very faint or in presence of a large number of different linear structures more distinct or longer than a real wake.

Therefore a number of different preprocessing algorithms were tested with the aim of increasing probability of detection and consequently reducing the probability of false alarm. Among the most beneficial methods are high-pass filtering removing large-scale contrast of the image, box averaging reducing speckle noise effect and non-linear amplification of the image intensifying the most prominent features. Results of their implementation are discussed in the last part of the paper.

2 THE RADON TRANSFORM

The main part of the algorithm consists in the implementation of the Radon transform on the test area.

The Radon transform in a continuous Euclidean space is usually defined as[3]:

$$f^*(\rho,\theta) \equiv \Re\{f\} = \iint_D f(x,y)\delta(\rho - x\cdot\cos\theta - y\cdot\sin\theta)dxdy, \tag{1}$$

in which D represents the entire image domain, $f(x,y)$ the function value at position(x,y), δ the Dirac delta function, ρ the normal distance between the origin and the line, and θ the angle between the normal and the x-axis. In our work, however, different coordinates are used to determine the position of the line:

$$f^*(s,i) \equiv \Re\{f\} = \frac{1}{\cos\alpha}\iint_D f(x,y)\delta[y - (s\cdot x + i)]dxdy, \tag{2}$$

where $s = \tan(\alpha)$, α is an angle between the line and x-axis, i the distance between the origin and intersection of the line with y-axis (see figure 1). Note that the weight function $\frac{1}{\cos\alpha}$ is necessary since its omitting leads to a *projection* of the line integral on the x-axis, resulting in non-correct Radon space performance.[3] Equation 2 can also be rewritten as a one-dimensional integral along a given line:

$$f^*(s,i) = \frac{1}{\cos\alpha}\int f(x, s\cdot x + i)dx. \tag{3}$$

An important difference of this representation is that the transformation of a single bright spot in the image space will give us the straight line in the Radon space rather than a sinusoidal one as in equation 1. Since we

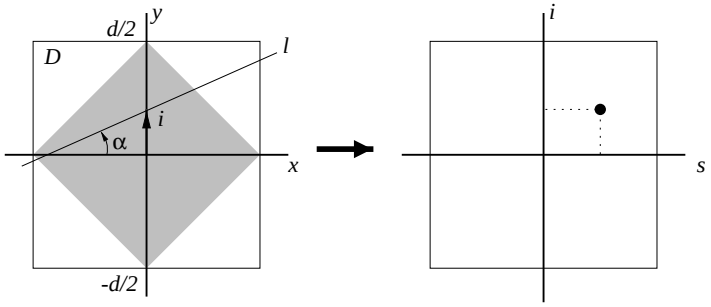

Figure 1: Radon transform configuration: (left) the space domain with a lineated structure l, (right) the corresponding position in the Radon domain

cannot consider Radon space to be infinite, the parameter i is limited between $[-d/2, d/2]$ so that only lines that intersect the shaded area in figure 1 can be calculated. This fact is of no importance for our purpose, however, since we applied an algorithm which places the ship in the center of the image.

In the case of SAR imagery, the function f is just a grey value of a pixel at the position (x,y). In equation 1, every linear feature in the image is mapped in the Radon space by integrating the amplitudes of every straight line and placing this integral as a single point in the transform space. This transform gives us two major advantages. First, all the bright pixels of the line are summarized at one spot, no matter how discontinuous the actual wake image will be[1]. Second, integration over lines not comprising any prominent structure averages out the intensity fluctuations. Therefore the signal-to-noise ratio of the wake extraction will be certainly higher in the transform

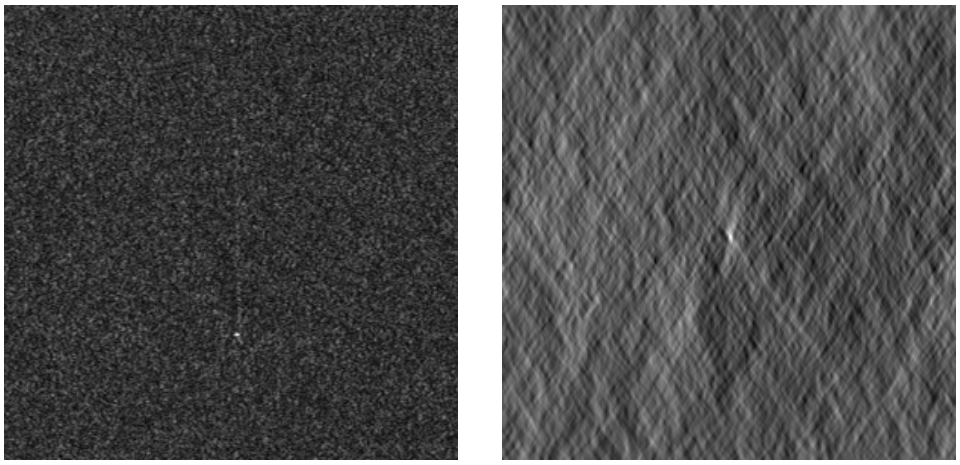

(a) SAR power image showing ship with wake

(b) The corresponding Radon domain

Figure 2: A SAR image and its Radon transform

space. In figure 2 the situation is shown in which a rather faint wake transforms into a quite clear spot in the Radon domain. Nevertheless, other structures may also show up in the Radon space.

3 DESCRIPTION OF THE ALGORITHM

In this paragraph, all the consequent steps of the algorithm performance (presented schematically in the figure 3) are described.

3.1 Identification and elimination of the ship

The first step in the automatic wake detection algorithm consists of thresholding the original image to localize the ship positions. For usual SAR-image the pixel values corresponding to the detectable ship are approximately five times higher than the average value of the whole scene. This difference is large enough to enable ship detection.

Connected components labeling was applied to the filtered image to calculate the center of mass of every ship as an isolated area of bright pixels linked to each other. This operation is performed for the proper elimination of extremely bright area around the center of a ship by replacing it with the mean value of the image amplitude. This is necessary as the areas corresponding to the ships are so bright that they would lead to the total disguise of any wake or linear structure, even after the integration process.

[1] For convenience we will further refer only to maxima, taking into account that every dark line can be transformed in a bright one by simple inverting the image

3.2 Localization of the Radon transform

After all ships are properly located and replaced by the mean value, windows of approximately 250×250 pixels centered around the ship's location were transformed into the Radon space. The size of the window which is extracted from the whole image is quite important as the Radon transform will be most efficient when the size of the window is about the size of the wake. The greater the window in comparison with the wake, the lower its signal-to-noise ratio. As most of the wakes that we encountered did not exceed several dozen pixels this size proved to be optimal. Choosing very small windows, even in case of very short wakes, is not efficient either since then we will lose the noise fluctuations reducing the averaging factor.

3.3 Selection of the local maxima

The idea of automatic wake detection (cf. figure 3) is based on sequentially detecting the maximum values in the Radon space, followed by their evaluation using certain criteria. In case of rejection of the highest maximum its value is replaced by zero and the next maximum is considered. This algorithm needs to be executed twice for every ship as in the ideal case we would expect the classical *V-shape wake* to be detected.

This procedure assumes that every maximum corresponds to a different line structure in the image. Practically, however, every line produces a cluster of bright pixels rather than a single point due to the non-zero width of the line. In order to avoid regarding two very close lines of one wake component as a *V-shape wake* we apply a filter to the Radon space which found out the maximum value in a small box and replaced all other pixels in it by zero values. This way the adjacent maxima could not be closer to each other than the size of the box which was chosen equal to 20 pixels by analyzing available wakes and the results of their detection by the program.

3.4 Criteria for ship wake detection

Among the criteria which were used for making a decision concerning wake presence in the image the most helpful proved to be *proximity* and *causality* criteria. These criteria are disscussed below together with other statistical parameters that can be of use.

3.4.1 Proximity criterion

The first criterion for distinguishing a real wake from other linear features consists in the verification of the evident fact that a wake must be located close to the ship. The offset can be easily estimated by calculating the Doppler shift produced by the ship movement with a probable speed exactly in the range direction[6]:

$$x = -\frac{u_r \cdot R}{V}, \tag{4}$$

where x is the offset value produced by the Doppler shift, u_r is the velocity of the vehicle in range direction, R is the distance between the vehicle and the sensor, and V is the velocity of the satellite. The value of x was taken equal to 20 pixels which corresponds to approximately 500 meters on the ground. In case of a greater offset the detected linear feature may be only a noisy structure or at least the wake of another ship. In case of satisfying this criterion the wake was subjected to the other statistical verification, otherwise the next maximum was considered.

As shown in tables 1 and 2, the number of wakes rejected by this criterion represented by the parameter N proves to be important in deciding if the linear structure is a wake or not. In fact, if we are dealing with

a well-prominent wake this number is most likely zero which—together with other statistical criteria—gives us quite reliable evidence of the wake presence. In case of a rejection of several maxima the decision is much more complicated. Moreover, in case of the rejection of several dozen first maxima it is most probably impossible to distinguish the wake from other structures, even if it is present. In the last case the level of noise is so high (see table 1, lowest part) that the difference in values of pixels of the wake—which is usually short and faint—are about the average noise variation. In this case some preprocessing techniques are necessary to increase signal-to-noise ratio of the wake.

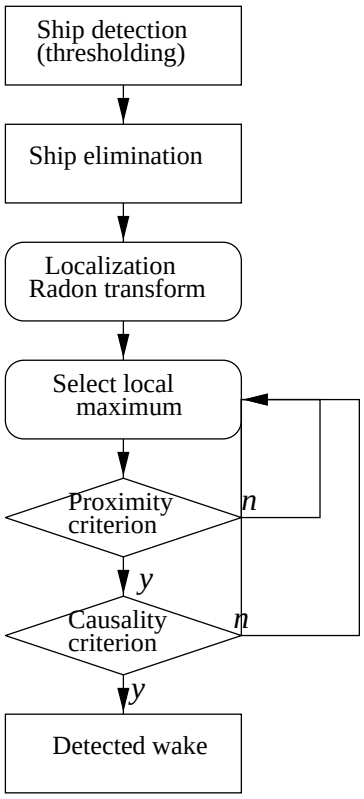

Figure 3: Ship wake detection flow chart. The straight boxes denote the space domain (SAR image), the rounded boxes the Radon domain.

3.4.2 Causality criterion

Another criterion used for wake recognition is based on the fact that a wake should be situated only at one side of the ship. The idea lies in the comparison of the average values of pixels belonging to two parts of the same line but located at different sides of the ship. Naturally, since the wake line does not cross the ship the division is performed using the intersection of the line with its normal at the ship's location. As the appearance of both wakes and images vary greatly, the difference threshold which would determine the wake presence can be selected only statistically, i.e. it should be derived from the analysis of the image area around the detected ship.

At first the standard deviation σ of the grey values of the selected part of the image without any visible

irregularities is calculated:

$$\sigma = \sqrt{\frac{\sum_{i=1}^{N}(x_i - \mu)^2}{N-1}}, \tag{5}$$

where x is the grey value of a pixel, μ the mean value of the window and N the number of pixels in the selected window. The standard deviations of the average values of two parts of the line μ_1 and μ_2 can be calculated then:

$$\sigma_{\mu_i} = \frac{\sigma}{\sqrt{N_i}}, \quad i = \{1, 2\}, \tag{6}$$

in which N_1 and N_2 are the numbers of points calculated as belonging to two parts of the line upon averaging procedure. The standard deviation of their difference is:

$$\sigma_{\mu_1 - \mu_2} = \sqrt{\sigma_{\mu_1}^2 + \sigma_{\mu_2}^2}. \tag{7}$$

If we assume now the hypothesis H_0 that $\mu_1 = \mu_2$, i.e. *there is no wake*, then this hypothesis will be rejected—leading to the conclusion that there is a wake present—in α percent cases when

$$R = \frac{\mid \mu_1 - \mu_2 \mid}{\sigma_{\mu_1 - \mu_2}} > K(\alpha). \tag{8}$$

The value of K in case of a normal distribution depends only upon α and can be taken from standard tables.[7] In case of $\alpha = 5\%$ it equals to $K(0.05) = 1.96$, which means that if we check all maxima on satisfying the criterion in equation 8 with $K = 1.96$, only the 5%-highest maxima will be considered as wakes. In practice, however, we are not dealing with randomly chosen maxima but with elements that were detected as the most prominent structures. Therefore the value of K should be higher; $K = 4.0$ or even 6.0. In the tables 1 and 2, the parameters R_1 and R_2 represent the values of R in equation 8 for the first and second "correct" maxima respectively.

3.4.3 Other statistical parameters

Other parameters presented in tables 1 and 2 describe how prominent the detected maximum is in comparison with other line integrals in the image. σ_r is the standard deviation of the Radon space multiplied with a factor 4 in analogy with the K parameter. The parameters $M_{1,r}$ and $M_{2,r}$ represent the differences between the first and second maximum value respectively and the average value μ_r of the image. They are presented to enable a comparison with σ_r. The case in which the value of M exceeds σ_r implies that we deal with a quite prominent linear feature. M and σ_r also characterize the noise level of the image when we know that there is no wake. Parameter S_r is defined by:

$$S_r = \frac{M_{1,r} - M_{2,r}}{Max_r - Min_r} \cdot 100\% \tag{9}$$

in which Min_r is the minimum and Max_r the maximum value in the Radon space. S_r represents how different (or significant) the first maximum is in comparison with the second. The last column is appointed for comments, whether the detected maximum is a wake or not.

4 PRELIMINARY RESULTS

Here we will analyse the results shown in table 1. This table is the result of a preliminary application of the described algorithms, so no preprocessing steps have been applied. The results are divided into three classes, corresponding to different states of the sea-surface that we encountered. The first class of images, **A**, is

Class	Nr.	R_1	R_2	σ_r	$M_{1,r}$	$M_{2,r}$	S_r	N	Wake/Noise
A	1	7.09	0.96	1.91	3.77	1.81	34.38	0	wake
A	2	4.71	0.64	1.85	2.89	2.07	17.43	0	wake
A	3	5.51	2.21	1.80	2.58	2.07	10.98	0	wake
A	4	4.56	1.21	1.89	2.21	1.95	6.35	0	wake
A	5	3.20	0.50	1.84	1.77	1.59	4.60	1	wake
A	6	1.57	0.86	1.87	1.67	1.65	0.67	15	noise
A	7	0.22	1.67	1.89	1.70	1.68	0.71	20	noise
A	8	1.06	2.30	1.89	1.76	1.64	3.18	12	noise
A	9	0.39	1.71	1.96	1.82	1.77	1.28	12	noise
A	10	0.23	0.27	1.94	2.01	1.78	5.66	7	noise
A	11	0.54	1.85	1.87	1.73	1.62	3.14	10	noise
B	1	12.32	1.00	17.34	30.34	18.11	24.83	0	wake
B	2	18.14	1.93	26.87	36.38	20.00	21.38	2	wake
B	3	5.08	0.37	23.57	26.22	24.11	3.58	8	wake
B	4	1.71	3.43	32.95	25.76	23.27	3.47	16	noise
B	5	0.97	6.46	18.03	16.38	16.27	0.25	21	noise
B	6	1.39	3.64	18.66	18.54	15.69	6.57	7	noise
C	1	4.11	3.26	2.06	1.75	1.49	6.36	12	wake
C	2	2.05	1.95	2.12	1.85	1.43	9.80	11	wake
C	3	0.03	0.21	2.10	1.64	1.53	2.50	19	wake
C	4	0.66	0.92	2.11	1.53	1.41	3.66	54	wake
C	5	0.79	0.13	2.33	2.08	1.68	8.40	6	noise
C	6	0.42	0.93	2.08	1.57	1.48	2.11	35	noise

Table 1: Preliminary results

characterized by rather favorable background conditions without any visible noisy linear structures, and cluttered only by speckle noise. The second class, **B**, represents a very noisy background with a much higher standard deviation and deflection from the normal distribution. In this case we still regard only very prominent or long wakes. The last class, **C**, consists of images with a rather noisy background and many non-wake linear features. Some of these non-wake linear features can be of artificial origin, produced by the preliminary compilation of the SAR data into the whole image. Moreover, in this case the wakes are very faint and practically not discernible without any preprocessing improvements. The results are organised in such an order that the first row ('number') of each group has the most prominent wake. The larger the number, the more faint or short the wake is. Regions containing only pure noise, as pointed out in the comment column, are also given for comparison.

Results for the first class of images are very promising. In spite of the fact that practically all considered wakes are quite faint and short they are well recognized by the value of R_1, which is exceeding three. Note that the average value of R for the all-noise regions much lower. The number of rejected maxima, described by N is zero for all wakes except for the poorest case (#5) of a very faint wake, which is also an indication of a low signal-to-noise ratio. The results showed us also that parameter S_r did not prove to be very relevant for wake recognition purposes, as it was presumed beforehand. Its value for noise-only regions and for not very distinct wakes were often about the same. Still, in cases of very prominent wakes S_r can take very high values (class **A**,#1,2 and **B**#1,2).

In the second class the background conditions were much worse. This can be easily seen by comparing the σ_r and M values with class **A**. For this class of images we still looked only at very prominent and long wakes (the size of the transformed area was also enlarged up to 400×400 pixels). In this situation all wakes were also well recognized. The problem for valid recognition here is that the images often show wakes that remained form ships that already left the area of interest. In such a noisy background it was practically impossible to reliably

detect 'real' wakes or their absence among the wakes of other ships crossing the image. An example of this effect can be observed in case **B**,#2: although the high value of $M_{1,r}$ clearly indicates the presence of a very prominent wake, the number of the rejected maxima N equals 2, which implies that there are some elongated structures which are even more prominent, or rather, longer than the detected wake. In case of a less prominent wake it will probably be very difficult to improve the situation by any preprocessing techniques, as both features of interest and noise elements are of the same nature. The same can be said about the presence of very dark and wide patterns produced by oil spill patches that can distort the image severely and make automatic wake detection more complicated.

In the third class, with very faint and usually short wakes, the wakes are not recognized (except the case of the longest wake) among the more prominent linear structures and the background noise. This situation is clearly indicated by the large number of rejected maxima N. Therefore we can conclude that this last class represents a problem for automatic wake detection. In the next section we will show how some preprocessing filters can increase the signal-to-noise ratio of the wakes.

5 PREPROCESSING FILTERS

In this part of the paper the results of some preprocessing filter applications will be discussed and some recommendations will be made.

Since most of the wakes in the images of class **C** are not prominent enough to be detected directly, different preprocessing filters are tested to improve this situation. The results of this filtering are presented in table 2. All the cases correspond to the same wakes as in class **C** in table 1, using the same numbering. The first part of the results represents application of image squaring (S) together with low-pass filtering (LP) performed by averaging within a running box. Applications of high-pass filtering (HP) performed in the Fourier space are given in the second part of the table. The third part is a combination of the first two cases. This results in band-pass filtering (BP) and squaring.

Although all the wakes are very faint we still expect that the average value of the pixels of a wake will be higher than the average value of the whole image, since otherwise they would not be detectable at all. Therefore it is reasonable to apply a non-linear amplification of the image to stress its most prominent features. In our case this was done by squaring, but also a third power may be appropriate. Higher powers usually lead to a practically binary image with an unacceptable high level of noise for reliable feature extraction.

Low-pass filtering by convolution using a running box is directed for speckle noise reduction as a result of averaging. This procedure is presumed to have little effect on a wake, as a wake usually presents a more prominent and organized feature. The best results were obtained applying a 3×3 box convolution. It should be mentioned that due to this operation a wake becomes more faint but wider. This way for calculating the μ values of the wake in equation 8, we should increase the parameter which determines how far a pixel can be located from the line to be still considered as belonging to the wake.

We can see that after applying these two operations together (table 2, part LP+S) all the wakes were detected by the program. However, the noise level also increased and the signal to noise ratio did not become very high. The comparison of the M values with a threshold level also indicates that the linear features are still very faint.

The high-pass filtering performed in the Fourier space (table 2, part HP), is performed to eliminate a certain kind of noise. Relatively large-scale fluctuations, that are sometimes not recognizable by visual analysis but are always present, can lead to a significant deterioration of the wake detection.[5] Their elimination, with an optimal cut-off frequency chosen equal to 0.05, led to increasing signal-to-noise ratio which can be verified by the significant reduction of the number of rejected maxima N.

Filter	Nr.	R_1	R_2	σ_r	$M_{1,r}$	$M_{2,r}$	S_r	N	Detection
LP+S	1	6.86	4.18	15.91	9.80	6.49	12.16	18	wake
LP+S	2	6.63	3.81	14.95	12.64	12.19	1.50	9	wake
LP+S	3	5.11	1.40	14.41	8.42	7.71	2.75	22	wake
LP+S	4	7.48	4.92	15.57	8.06	6.13	7.50	38	wake
LP+S	5	4.12	2.04	15.25	10.65	10.53	0.37	20	wake
LP+S	6	3.03	0.60	16.13	10.78	10.01	1.69	16	noise
HP	1	4.24	0.81	5.48	6.31	5.95	2.73	1	wake
HP	2	2.39	1.57	6.42	6.23	6.00	1.67	3	noise
HP	3	0.79	0.41	6.53	7.58	6.70	5.51	1	noise
HP	4	0.33	1.47	6.41	5.92	5.35	4.25	11	noise
HP	5	0.63	0.70	5.57	6.07	5.48	4.86	3	noise
HP	6	1.69	1.02	5.53	4.76	4.65	0.96	28	noise
BP+S	1	10.90	3.51	10.45	12.51	9.87	10.75	2	wake
BP+S	2	6.61	3.07	10.44	12.12	10.24	7.69	2	wake
BP+S	3	6.58	0.66	10.25	9.91	9.82	0.38	6	wake
BP+S	4	4.58	1.06	10.43	11.36	9.03	9.33	1	wake
BP+S	5	1.95	2.58	10.42	10.01	8.72	5.35	27	noise
BP+S	6	4.39	3.53	10.58	10.45	9.00	6.25	4	wake

Table 2: Results after preprocessing filtering. LP: low-pass filter, HP: high-pass filter, BP: band-pass filter, S: squaring

Optimal results are obtained by applying all the described filters to the same image (table 2, part BP+S). We can see that all the wakes were recognized with their maxima prevailing the standard deviation value multiplied by factor 4, except for the poorest case. Still, if we are dealing with a very high noise level and a number of rejected maxima greater than zero, the algorithm can provide only an essential contraction of the field of search and detection of the present wakes but not their reliable recognition among the other features. Therefore, the success of the algorithm implementation depends greatly upon the kind of imagery it was appied to. Therefore it could be necessary to sort out the images to select ones that can be treated automatically. Probably, this can be also be performed in an automatic procedure.

For some cases more sophisticated algorithms need to be applied for the elimination of very disturbing kinds of noise, i.e. for removing regular linear patterns produced by the SAR image compilation. Elimination of linear structures that cross the whole image and which are connected with none of the present ships will probably also be a useful procedure.

6 CONCLUSIONS

The success of the automatic wake recognition algorithm depends greatly upon the quality of the SAR scenes it was applied to. Therefore, preliminary image sorting is necessary to divide the images that can or cannot be treated automatically. Three types of situations that we encountered can be described.

1. The first is the situation of a quite favorable background condition withou any kind of noisy linear structures. In this case the application of the algorithm is very promising. Even very short and faint wakes are easily recognized with a very low false alarm rate.

2. In case of a very noisy background, prominent or relatively long wakes are also easily detected and distinguished from noise elements.

3. Very faint and short wakes in rather noisy background cluttered with a great deal of different linear features cannot be recognized by simple applying the Radon transform.

Application of band-pass filtering together with non-linear amplification of the image can significantly contribute to the wake detection algorithm results, even in case of very faint wakes. Nevertheless, reliable wake recognition in a scene with different linear features still remains, even in this case, rather complicated.

7 REFERENCES

[1] A C Copeland, G Ravichandran, and M M Trivedi. Localized Radon transform-based detection of ship wakes in SAR images. *IEEE Transactions on Geoscience and Remote Sensing*, 33(1):35–45, January 1995.

[2] R C V Feron, R A Hartmann, H J den Hollander, and L P M van der Meij. Marine traffic monitoring with ERS-1 SAR images; a feasibility study. Technical Report MD/GAR 9547, Survey Department of the Directorate–General, 1995. 29 pages.

[3] R H Hanssen. The application of Radon transformation for improved analysis of sparsely sampled data; a feasibility study. Technical Report 93.1, Delft University of Technology. Report of the Faculty of Geodetic Engineering, Mathematical and Physical Geodesy, December 1993.

[4] A K Liu, C Y Peng, and Y S Chang. Mystery ship detected in SAR image. *EOS, Transactions, American Geophysical Union*, 77(3):17–18, January 1996.

[5] M Y Rey, J K E Tunaley, J T Folinsbee, P A Jahans, J A Dixon, and M R Vant. Application of Radon transform techniques to wake detection in Seasat-A SAR images. *IEEE Transactions on Geoscience and Remote Sensing*, 28(4):553–560, July 1990.

[6] I S Robinson. *Satellite oceanography: An introduction for oceanographers and remote-sensing.* Ellis Horwood series in marine science. Horwood, Chichester, 1985.

[7] R B G Williams. *Introduction to Statistics; for Geographers and Earth Scientists.* MacMillan, London, 1984.